

anticipated seasonal variation in the zonal wind field of the stratosphere presents a more complex situation, and we will not attempt to analyse the requisite angular momentum transports.

### Conclusions

IR brightness temperature at  $200\text{ cm}^{-1}$ ,  $530\text{ cm}^{-1}$ , and  $1,304\text{ cm}^{-1}$  exhibit small meridional contrasts ( $\leq 3\text{ K}$ ) in the troposphere and tropopause region and larger contrasts ( $\sim 20\text{ K}$ ) in the upper stratosphere. Radiative relaxation times estimated for the troposphere and stratosphere are large compared with the length of Titan's day. In the lower troposphere they are also large compared with the length of a season,  $\Omega_s \tau_R \gg 1$ , implying a lack of seasonal variation in temperature. In the upper stratosphere,  $\Omega_s \tau_R \ll 1$ , and seasonal variations in temperature should be large. The location of the transition region, where  $\Omega_s \tau_R = 1$ , is not well determined.

The absence of detectable longitudinal structure in the observations suggests that baroclinic waves and eddies are absent in Titan's atmosphere. Zonally symmetric flows are the

preferred mode of meridional heat transport and thermally driven planetary-scale circulations yield characteristic meridional velocities of  $0.04\text{ cm s}^{-1}$  in the lower troposphere and  $5\text{ cm s}^{-1}$  in the upper stratosphere.

The observed meridional temperature contrasts imply zonal winds which are cyclostrophic, reaching  $\sim 100\text{ m s}^{-1}$  in the upper stratosphere. The anticipated seasonal variation in the stratospheric temperature field implies a concomitant variation in the zonal winds at high altitudes. The inferred cyclostrophic flow has an angular momentum per unit mass which, at least in the stratosphere, greatly exceeds  $\Omega a^2$ . In the lower troposphere, an assumed balance in the vertical transport of angular momentum by zonally symmetric meridional flow and down gradient diffusion implies a vertical viscosity of only  $10^3\text{ cm}^2\text{ s}^{-1}$ .

We thank V. G. Kunde for gaseous transmittance tables for Titan's stratosphere, W. C. Maguire for helpful discussions, also M. E. Geller, P. J. Gierasch, C. B. Leovy and R. A. Hanel for their critical reading of the manuscript.

Received 18 June; accepted 20 July 1981.

1. Samuelson, R. E., Hanel, R. A., Kunde, V. G. & Maguire, W. A. *Nature* **292**, 688–693 (1981).
2. Hanel, R. et al. *Science* **212**, 192–200 (1981).
3. Smith, B. A. et al. *Science* **212**, 162–190 (1981).
4. Gierasch, P. J., Goody, R. M. & Stone, P. H. *Geophys. Fluid Dyn.* **1**, 1–18 (1970).
5. Harshvardhan & Cess, R. D. *Tellus* **28**, 1–9 (1976).
6. Tyler, G. et al. *Science* **212**, 201–206 (1981).
7. Strobel, D. F. in *Atmospheres of Earth and the Planets* (ed. McCormac, B. M.) 401–408 (Reidel, Dordrecht, 1975).
8. Hess, S. L. *Introduction to Theoretical Meteorology* (Holt, Rinehart and Winston, New York, 1959).
9. Carlson, B. E., Caldwell, J. & Cess, R. D. *J. atmos. Sci.* **37**, 1883–1885 (1980).
10. Prabhakara, C., Rodgers, E. B., Conrath, B. J., Hanel, R. A. & Kunde, V. G. *J. geophys. Res.* **81**, 6391–6399 (1976).
11. Schubert, G. et al. *J. geophys. Res.* **85**, 8007–8025 (1980).
12. Held, I. M. & Hou, A. Y. *J. atmos. Sci.* **32**, 1038–1044 (1975).
13. Leovy, C. B. & Pollack, J. B. *Icarus* **19**, 195–201 (1973).
14. Stone, P. J. *atmos. Sci.* **32**, 1005–1016 (1975).
15. Brinkman, A. W. & McGregor, J. *Icarus* **38**, 479–482 (1979).
16. Lorenz, E. N. *The Nature and Theory of the General Circulation of the Atmosphere* World Meteorological Organization (1967).
17. Cess, R. D. & Caldwell, J. *Icarus* **38**, 349–357 (1979).
18. Geller, M. A. *J. atmos. terr. Phys.* **41**, 683–705 (1979).
19. Dunkerton, T. J. *atmos. Sci.* **35**, 2325–2333 (1978).
20. Schneider, E. K. *J. atmos. Sci.* **34**, 280–296 (1977).
21. Gierasch, P. J. *J. atmos. Sci.* **32**, 1038–1044 (1975).
22. Rossow, W. B. & Williams, G. P. *J. atmos. Sci.* **36**, 377–389 (1979).
23. Leovy, C. B. *J. atmos. Sci.* **30**, 1218–1220 (1973).
24. Stone, P. H. *J. atmos. Sci.* **31**, 1681–1690 (1974).

## Implications of Titan's north-south brightness asymmetry

Lawrence A. Sromovsky\*, Verner E. Suomi\*, James B. Pollack†, Robert J. Krauss\*, Sanjay S. Limaye\*, Tobias Owen‡, Henry E. Revercomb\* & Carl Sagan§

\* Space Science and Engineering Center, University of Wisconsin-Madison, Madison, Wisconsin 53706, USA

† NASA Ames Research Center, Moffett Field, California 94035, USA

‡ Department of Earth and Space Sciences, SUNY at Stony Brook, Stony Brook, New York 11790, USA

§ Laboratory for Planetary Studies, Cornell University, Ithaca, New York 14853, USA

*Voyager 1 images of Titan, when normalized to remove limb darkening, reveal an axially symmetric brightness pattern with significant north-south asymmetry. This interhemispheric contrast seems to be a response to seasonal solar heating variations resulting from Titan's inclined spin axis. The contrast significantly lags the solar forcing, indicating that its production involves the atmosphere well below the unit optical depth level. The contrast has a significant effect on Titan's disk-integrated brightness as seen from Earth, and probably accounts for most of the observed long term variation, with solar UV variations accounting for the remainder.*

EARTH-based observations<sup>1,2</sup> show that between 1972 and 1976 Titan's disk-integrated brightness increased by  $\sim 9\%$  in the blue (b) and  $\sim 5.5\%$  in the yellow (y) to a maximum during 1976–77, and decreased through 1978. This variation and a similar but smaller variation in Neptune's brightness can be correlated with the solar cycle<sup>2,3</sup>, suggesting solar variability as the common cause. As photochemical reactions are thought to produce the submicrometre aerosols in both atmospheres, we expect the variation in solar UV output during the solar cycle<sup>4,5</sup> to affect the amount or physical properties of the aerosols. Pollack *et al.*<sup>6</sup> showed that Titan's brightness changes during 1972–76 could be produced by changes in mean particle size, visible absorption coefficient, or optical depth, and that the fractional decrease in the particle production rate required to explain the increase in albedo was roughly consistent with the estimated fractional change in solar UV output.

A new mechanism for explaining at least part of the Earth based photometry of Titan is suggested by the Voyager 1

observations of November 1980 that showed Titan to be shrouded in an apparently unbroken cloud cover with several large-scale zonal features and a surprising north-south asymmetry in brightness<sup>7</sup>. As Titan's spin axis is inclined  $27^\circ$  to the ecliptic (assuming Titan is tidally locked to Saturn), the angle between Titan's axis and the line of sight to the Earth varies during Saturn's (and Titan's) 29.5-yr orbit around the Sun. The apparent tipping motion, combined with the brightness asymmetry could result in a long-term periodic variation of Titan's disk-integrated brightness. If the brightness asymmetry also varies in response to seasonal changes in solar heating of the deepest layers of the atmosphere<sup>7</sup>, then the contrast would follow the seasonal heating asymmetry with a phase shift of nearly a full season and would reach an extreme value near Titan's equinoxes (near the time of the Voyager 1 encounter). Using a highly simplified model to combine the effects of the suggested seasonal changes in contrast and the time-dependent viewing conditions, the predicted brightness variation is found

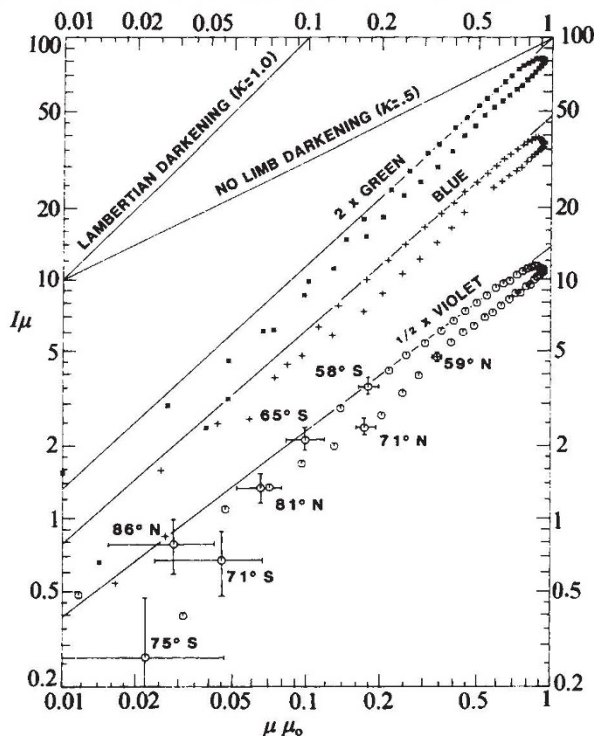


**Fig. 1** Voyager 1 intensity measurements in violet, blue, and green filters, along Titan's 150° E meridian. Lines drawn for each colour show the Minnaert fits to intensities between 31° and 52° S. Intensities (in digital counts) have been corrected for dark noise but not converted to absolute units. The error bars labelled by latitude show the effects of an intensity uncertainty of  $\pm 0.5$  count and an uncertainty in  $\mu$  and  $\mu_0$  corresponding to a  $\pm 1$  pixel error in the image location of Titan's centre. The identification of image line and element coordinates with Titan latitude and longitude, image navigation, is based on predicted spacecraft location and attitude information supplemented by a precise determination of camera pointing derived from the location of Titan's centre within the image.

to be in phase with the Earth-based photometry and within a factor of 2 of the observed magnitude change<sup>7</sup>.

The essential differences between the solar cycle and seasonal components are the driving forces and the response times. The former is driven by the changing UV output of the Sun, and brightness changes in the same direction would be expected at all latitudes at the same time, with a delay of the order of six months relative to the UV forcing function<sup>8</sup>. The seasonal component is driven by the tipping of Titan's axis relative to the Sun, causing simultaneous brightness changes in different directions in northern and southern hemispheres, with a time lag of nearly a full season ( $\sim 7$  yr). In both cases, the properties of the aerosol particles are probably modulated and in turn produce the observed brightness changes.

We now use Voyager 1 and Pioneer 11 observations, with recent Earth-based photometry, to place firmer bounds on the phase shift of Titan's contrast relative to the seasonal forcing. Describing the contrast in terms of a relative normal albedo, we calculate the time dependence of Titan's disk-integrated brightness and find a significant seasonal contribution. Finally, we use the spectral and phase angle dependence to place constraints on the mechanism which produces the contrast.

#### Titan's brightness contrast at the time of Voyager 1

We selected nearly simultaneous Voyager narrow angle frames in violet (0.37–0.45  $\mu\text{m}$ ), blue (0.43–0.53  $\mu\text{m}$ ), and green (0.52–0.60  $\mu\text{m}$ ) filters (A. Collins, P. Kupferman and E. Danielson, personal communication), pictures 1305S1–003, 1289S1–003, and 1287S1–003 respectively. These were taken at  $2.38 \times 10^6$  km from Titan, at a phase angle of 29.6°, with a resolution of 44 km per line pair at the subspacecraft point. The Voyager blue and green intensities roughly correspond to Lockwood's measurements with the b filter (0.45–0.48  $\mu\text{m}$ ) and y filter (0.54–0.56  $\mu\text{m}$ ) respectively<sup>3</sup>. Relative intensities were obtained from raw digital counts by subtracting an empirically determined dark noise correction accurate to  $\sim \pm 0.5$  count.

To define limb darkening characteristics each image was scanned along the 150° E meridian, using a  $5 \times 5$  pixel area average stepped at  $\sim 3^\circ$  intervals (Fig. 1). These scans pass between the subspacecraft point at 134° E and the subsolar point at 162° E, providing nearly maximal variation in scattering geometry and intensity. Figure 1 shows the dependence of intensity  $I$  (in digital counts) on  $\mu$  (cosine of the observer zenith angle) and  $\mu_0$  (cosine of the solar zenith angle) as  $I\mu$  versus  $\mu\mu_0$  on logarithmic scales so that Minnaert scattering behaviour, for which

$$I\mu = I_0(\mu\mu_0)^k \quad (1)$$

is a straight line with slope equal to the limb darkening exponent  $k$ , and intercept (at  $\mu\mu_0 = 1$ ) equal to the maximum intensity  $I_0$ . Each scan follows two nearly linear traces with similar slopes, moving along one line in the northern hemisphere and a second line, with an intercept  $\sim 25\%$  greater, in the southern hemisphere. A transition occurs near the equator. Because roughly the same limb darkening slope applies over most of the latitude range for each colour, we can interpret brightness differences as differences in the intercept  $I_0$  (proportional to the normal albedo).

We define a latitude dependent relative normal albedo (Fig. 2) as the ratio of the observed intensities to the intensities predicted from a Minnaert function fit to the 150° E scan data between 31° and 52° S for each colour. The fitted slopes are 0.773, 0.887, and 0.942 for violet, blue, and green respectively. Four major cloud zones are apparent in Fig. 2: a north mid-latitude zone between about 10° and 55° N, a north polar zone between 55° and 90° N, a south mid-latitude zone between about 20° and 60° S, and an equatorial transition zone between about 20° S and 10° N. The large variations poleward of 60° S and 80° N cannot be interpreted as true variations in normal albedo as they occur where the determination of the viewing geometry is very sensitive to navigation errors (Fig. 1) and where the Minnaert function does not accurately describe Titan's limb darkening. The normal albedo of the south mid-latitude zone is  $\sim 25\%$  greater than that of the north mid-latitude zone, while the albedo of the north polar zone is  $\sim 7\%$  smaller. The greatest normal albedo contrast between the south and north mid-latitude zones occurs in the blue, and the smallest in the green.

The large-scale spatial structure of the normal albedo, as well as subtler cloud features are displayed as normalized images (Fig. 3) in which the intensity is proportional to relative normal albedo. The images clearly show the major cloud zones, and indicate a slightly brighter band at 45° N as identified by Smith *et al.*<sup>7</sup>. The features in the normalized images are primarily zonal (axially symmetric). The north polar zone is dark in all three colours, but darkest in violet. The bright band just south of this zone is most pronounced in the green and nearly invisible in the

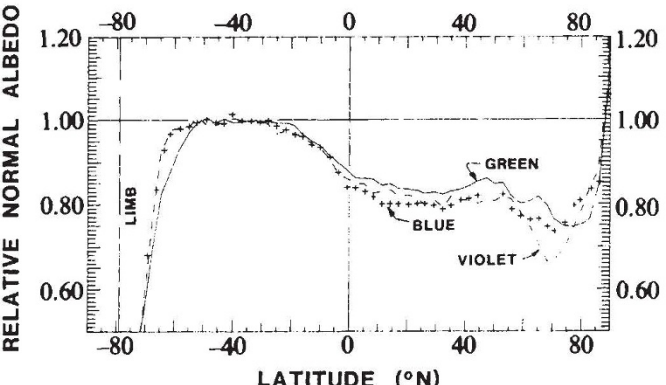


**Fig. 2** Relative normal albedo versus latitude along the 150° E meridian. For each colour the relative normal albedo is obtained by dividing observed intensities by predictions based on Minnaert fits to the intensities between 31 and 52° S. The increase of normal albedo north of 70° N is not real: a decrease similar to that near 70° S is found when  $\mu$  and  $\mu_0$  in the polar zone are corrected for the larger height of the clouds there. The decrease near the limb in the south is similar to that found near the limb at other latitudes and is probably a failure of the Minnaert fit to describe the true limb darkening at large viewing angles.

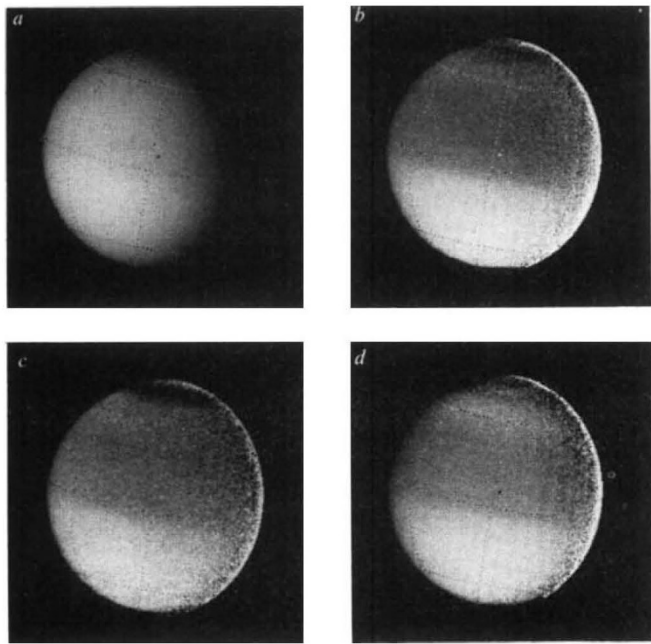


**Fig. 3** Voyager 1 narrow angle images of Titan at 29.6° phase angle: unnormalized blue image (*a*) and normalized images in blue (*b*), violet (*c*), and green (*d*). In all the normalized images intensities are linear in relative normal albedo (see text) but stretched to enhance the visibility of the relatively small contrast range. A similar linear stretch has been applied to the unnormalized image (*a*). Its different appearance is primarily due to the presence of limb darkening. The latitude-longitude grid overlay has a 45° spacing. The equator intersects the 135° E meridian near the centre of the image (+, Titan's centre). The bright terminator in the normalized images probably results from the haze layer above the main cloud deck<sup>7</sup>, which could cause the observed intensities to fall off more slowly than the predicted intensities, yielding an apparent albedo increase.

violet. Minor, but definite, longitudinal variations also occur. The north polar zone boundary, for example, is slightly inclined relative to latitude lines. The green image also shows an inclined bright feature within the polar zone which may be useful as a tracer of atmospheric motions. Those small departures from axial symmetry have an insignificant effect on Titan's disk-integrated brightness and are ignored.

### Phase angle dependence

We assume that the normal albedo contrast is the same at 0° phase angle (corresponding to Earth-based observing geometry) as it is at the 29.6° phase angle applicable to the Voyager 1 data shown in Figs 1–3. To test this assumption we analysed a Voyager 1 blue filter image taken at a phase angle of 9.3° (picture 1379S1-014), using the same procedures as in the analysis of the 29.6° phase angle images. No discernible change in mid-latitude contrast was found between these phase angles. The small size of the 9.3° phase angle image (30 picture elements across Titan's diameter) precludes a definitive statement about polar region changes.

### Time dependence of Titan's contrast

The possible time dependence of Titan's brightness contrast can be constrained by comparing the Voyager 1 and Pioneer 11 observations (1.17 yr apart). We used a blue filtered image made by the Pioneer 11 imaging photopolarimeter (IPP) at a phase angle of 27° and at a surface resolution of ~170 km at the subspacecraft point (M. G. Tomasko, personal communication). The spectral range of the IPP blue filter (0.39–0.50 μm) covers both the blue and violet bands of the Voyager camera system. Because we see little spectral dependence of contrast in this spectral range, and as the albedo of Titan is higher in the blue than in the violet, we expect no significant spectral error in comparing the IPP image with the Voyager blue image.

Using the same procedures as above, a central meridian scan of the IPP image was used to define the relative normal albedo as a function of latitude. The large quantization noise in the IPP

data was reduced by averaging over two latitude belts in which the normal albedo seemed to be constant: 15°–35° S and 30°–60° N. We found a south/north normal albedo ratio of  $1.26 \pm 0.03$  for the Pioneer measurements, compared with  $1.25 \pm 0.01$  for Voyager. This result is consistent with either a fixed contrast or a slowly varying contrast near an extremum. We reject the former possibility because it implies brightness variations grossly inconsistent with the Earth-based photometry. The Pioneer 11/Voyager 1 comparison also suggests that the normal albedo boundary (the point at which the albedo is midway between the mid-latitude values) has moved from about 5° N to 5° S, apparently opposite to the subsolar point. But this tentative result is not included in our seasonal model calculations.

If the contrast slowly varies with a seasonal period (29.5 yr), then the direct observations by Voyager 1 and Pioneer 11 place a strong constraint on the phase shift between the solar forcing due to spin axis tipping and the contrast response. If both the forcing and the contrast response vary sinusoidally, the implied phase shift is  $-84^\circ \pm 20^\circ$ , where  $-90^\circ$  corresponds to a time delay of one season, and the implied maximum south/north ratio of normal albedos is  $1.26^{+0.05}_{-0.01}$ . The relatively large uncertainty in phase is due to the small time interval between Voyager and Pioneer and the large quantization noise in the Pioneer results. Present results are consistent with maximum contrast near the time of the Voyager 1 encounter and allow for a large enough phase lag (near 90°) to place the contrast-induced brightness variation in phase with the Earth-based photometry.

If the normal albedo response to the solar irradiance level can be described by a single time constant, then the phase shift is determined by  $\tan(\phi) = -2\pi\tau/T$ , where  $\phi$  is the phase shift,  $T$  is the orbital period of Saturn, and  $\tau$  is the time constant. As  $\phi \leq -90^\circ$  is not physically possible, the time constants consistent with the phase shifts allowed by the Pioneer 11/Voyager 1 comparison fall in the range  $9.6 \text{ yr} \leq \tau \leq \infty$ , with the central phase shift of 84° corresponding to a time constant of 44.7 yr. This range of time constants is not consistent with a direct interaction between solar irradiance and aerosol properties at the unit optical depth level (at a pressure of ~1 mbar), because the thermal radiative time constant at this level and the time to reach equilibrium particle properties<sup>8</sup> are both <1 yr. Large time constants can be obtained, however, if deeper levels of the atmosphere are involved in the contrast producing mechanism. For the entire atmosphere down to the 1.6-bar level a time constant of 138 yr (ref. 7)  $\phi = -88^\circ$  is possible. A time constant of 9.6 yr only requires involvement down to the 100 mbar level.

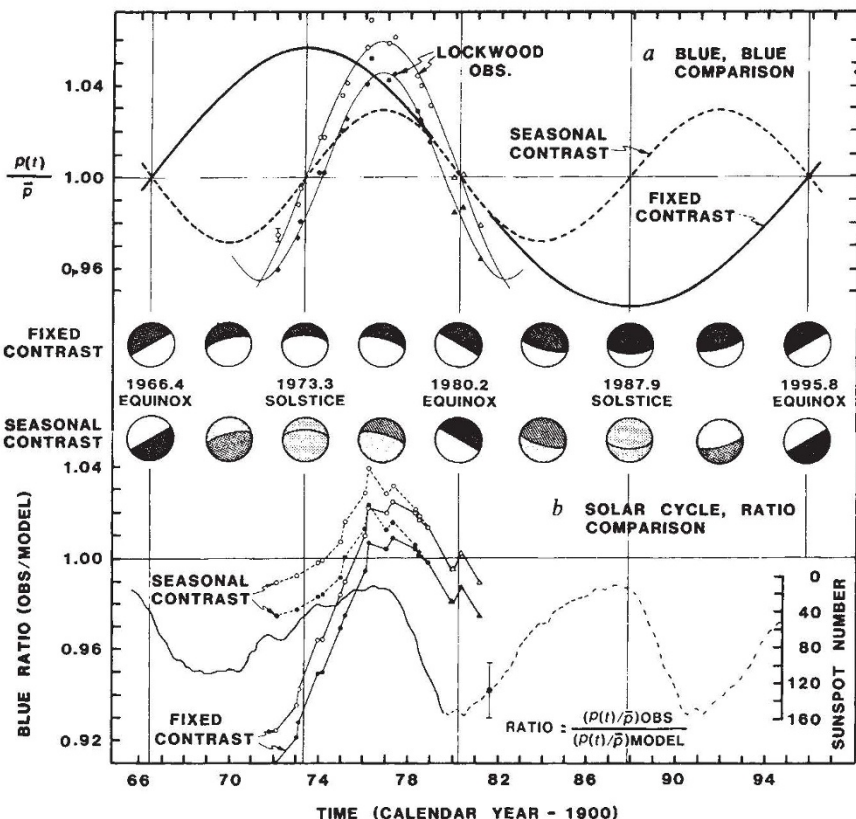
### Predicted geometric albedo time dependence

We now evaluate the time dependence of Titan's disk-integrated brightness expected for two models consistent with the Pioneer 11/Voyager 1 comparison: fixed contrast and seasonal contrast with a large phase shift ( $-90^\circ$  for this example). Because the Earth-based observations of Titan's disk-integrated brightness<sup>1,2</sup> have been adjusted to fixed heliocentric distance and zero phase angle (180° scattering angle), they are proportional to Titan's geometric albedo (the ratio of disk-integrated brightness to that of a flat perfect Lambertian reflector of the same diameter). We calculate the relative geometric albedo  $p(t)$  by integrating over the illuminated hemisphere:

$$p(t) = (1/\pi) \int \int a(\theta, t) [\mu_0(\theta, \theta_s(t), \phi)]^{2k} \sin(\theta) d\theta d\phi \quad (2)$$

where  $a(\theta, t)$  is the relative normal albedo at co-latitude  $\theta$  and time  $t$ ,  $\theta_s$  is the co-latitude of the subsolar (and subEarth) point, and  $\phi$  is the longitude relative to the subsolar longitude. The time dependence of the subsolar point latitude on Titan is obtained by assuming Titan's spin axis is parallel to Saturn's. We approximate the latitude dependence of the normal albedo using a 16-zone step function with boundaries spaced ~10° in latitude. Average relative albedo values for each zone are calculated for each colour from the results shown in Fig. 2. Because of the navigational and Minnaert fit uncertainties we

**Fig. 4** *a*, Relative time variation of Titan's blue geometric albedo according to fixed contrast (heavy solid line) and seasonal contrast (heavy dashed line) models. Relative time variations derived from Lockwood's Earth-based photometry are shown for two different estimates of the mean brightness, each based on fitting an offset sine function of fixed period to the observations. One case uses the 11-yr solar cycle period; the second uses the current 13.8-yr period of the predicted seasonal brightness variation (the ellipticity of Saturn's orbit causes a deviation from the mean 14.7-yr period). Both fits (light lines) are good: r.m.s. deviations from the fitted curves are only about 1.5 times the estimated measurement error. Observations:  $\square\Delta$ , relative to the mean assuming a 13.8-yr period;  $\bullet\Delta$ , relative to the mean assuming an 11-yr period. Triangles indicate observations which are still preliminary. The shaded drawings illustrate the time-dependent appearance of Titan at zero phase angle according to the two contrast models. The drawings exaggerate and simplify the contrast for clarity. *b*, Comparison of the solar cycle of smoothed sunspot number<sup>11</sup> with the ratio of observed to predicted relative variations in Titan's blue geometric albedo. Sunspot numbers are plotted along an inverted scale. The dashed portion of the sunspot curve indicates predicted behaviour based on previous cycles. The error bar indicates short term prediction uncertainty. Beyond 1983 the uncertainty is comparable with the predicted value.



assume the same albedo south of  $60^\circ$  S as between  $52.5^\circ$  S and  $60^\circ$  S, and ignore variations north of  $85^\circ$  N in finding a mean between  $70^\circ$  and  $90^\circ$  N. This normal albedo distribution is valid for 1980.9, the time of the Voyager 1 encounter. The fixed contrast model assumes the same distribution at all times. We describe possible seasonal variations in normal albedo in a simple model assuming (1) the normal albedo distribution for 1980.2 (the time of the last equinox) was the same as observed by Voyager for 1980.9, (2) the distribution for 1966.4 (time of the previous equinox) was as for 1980.2 except for a north-south reversal, and (3) at each latitude the normal albedo varied sinusoidally between the 1966.4 and 1980.2 extremes.

For fixed albedo contrast we find peak-to-peak modulation amplitudes of  $\sim 10.5\%$  for violet and blue geometric albedos, and  $8.2\%$  for the green. For seasonally-varying contrast the corresponding values are  $5.6\%$  and  $4.2\%$  respectively. Figure 4*a* illustrates the time dependence of the geometric albedo based on the normal albedo models for the blue intensities. For fixed albedo contrast,  $p(t)$  varies in phase with the subsolar motion, reaching extreme values at the solstices. For the seasonal contrast model,  $p(t)$  attains its mean value at every equinox, when both hemispheres are equally illuminated and viewed, and at every solstice, when the interhemispheric normal albedo contrast is absent. In this case the extreme values occur midway between solstice and equinox. The shaded drawings (Fig. 4*a*) provide a simplified illustration of Titan's time dependent appearance according to these two contrast models.

### Comparison with Earth-based photometry of Titan

The Lockwood measurements of Titan's *b* magnitude are plotted in Fig. 4*a* as relative brightnesses (brightness/time-averaged brightness). The most recent observations should be considered preliminary (G. W. Lockwood, personal communication).

The brightness variation calculated assuming a fixed normal albedo distribution is completely at odds with the Earth-based photometry. The predicted brightness is at a maximum in 1973 and beginning to decline, while the measurements are near the estimated mean value and rapidly increasing. This implies that the mean normal albedo of Titan's clouds and the relative albedo distribution with latitude cannot both be time-indepen-

dent. If the relative spatial distribution of normal albedo were fixed, then the disk-averaged mean value would have to vary dramatically to compensate as in Fig. 4*b*, which shows the ratio of Lockwood's blue observations to the predictions. As the ratio (for fixed contrast) changes most dramatically before 1976 when solar indicators (such as sunspot number, Fig. 4*b*) are changing relatively slowly, the possibility of fixed contrast and a large compensation by the solar UV mechanism seems highly unlikely.

If the relative latitudinal variation of normal albedo has the seasonal model time dependence, the predicted geometric albedo variation has roughly the same modulation period and phase as the Earth-based measurements. The assumed seasonal phase lag of  $90^\circ$  provides nearly optimal agreement with the Earth-based *b* brightness variation (Fig. 4*a*), although the optimal phase lag for fitting both *b* and *y* brightness curves is  $82^\circ \pm 7^\circ$ , where the uncertainty is based on the difference between best fit values for the two colours. The predicted peak-to-peak modulation amplitude based on the green contrast measurements is  $\sim 50\text{--}70\%$  of the observed *y* brightness modulation, while the predicted blue variation is about  $50\text{--}60\%$  of the observed *b* brightness modulation, where the amplitude uncertainties are due to the uncertainties in Titan's mean brightness. For agreement with the Earth-based photometry the mean normal albedo can be modulated by only  $\sim 5\%$  in blue and only  $2.5\%$  in the green (or *y* filter). This implied variation in disk-averaged mean normal albedo (Fig. 4*b*) is roughly in phase with that expected from the solar cycle modulations of UV output (Fig. 4*b*), although the magnitude of the solar cycle effect in the present case would be only about half the amount suggested before Titan's brightness contrast had been discovered.

### Implications of Neptune's brightness variation

The seasonal contribution to Titan's brightness variation could be significantly different from the above estimate if the boundary between high and low albedo also exhibited seasonal variation: it would be greater if the boundary moved opposite to the subsolar point motion (as suggested by Pioneer 11 measurements) and smaller if it moved in the same direction.

Thus dominance by either solar cycle or seasonal contributions remains possible. Earth-based photometry of Neptune is helpful in evaluating this possibility.

As Neptune's orbital period of 164.8 yr seems to preclude any significant seasonal changes during the 1972–80 period of the Earth-based photometry, we might expect its brightness curve to be dominated by the solar UV mechanism. The asymmetric form of Neptune's brightness variation supports this expectation: after relatively smooth increases between 1972 and 1976.5, at an average rate of  $0.54\% \text{ yr}^{-1}$  in the blue and  $0.68\% \text{ yr}^{-1}$  in the yellow, the brightness curves for both colours dropped by more than 2% in the yellow and almost 3% in the blue within the next year, with relatively little additional change from 1978 to 1980 (ref. 2 and G. Lockwood, personal communication). Thus Neptune's brightness curves are relatively well correlated with the asymmetric variation of the indicators of solar activity (Fig. 4b).

If the shape of Neptune's brightness curve represents the relative time dependence of the solar cycle contribution to Titan's brightness, then the solar cycle mechanism cannot be dominating Titan's variation. The very symmetric form of Titan's brightness curve is instead consistent with dominance by the seasonal mechanism. However, between 1972 and 1976 Titan's b magnitude increased  $\sim 70\%$  faster than the y magnitude, while between 1976 and 1980 they both changed at about the same rate. We interpret this spectral difference as evidence for a non-seasonal component. From the amplitude of Neptune's brightness variation we infer that the solar cycle component in Titan's brightness curve would contribute  $\sim 30\%$  of the total variation. Although one might expect a larger effect because Titan's haze layer is optically thick, while Neptune's is thought to be optically thin, a contribution much greater than 30% should produce a noticeable asymmetry in Titan's brightness curve. Thus a simple seasonal component probably accounts for more than half of Titan's secular variation, with the remainder being provided by the solar cycle mechanism.

### Constraints on the contrast mechanism

As most photons reflected to space by Titan interact with the atmospheric aerosols, the hemispheric brightness asymmetry is almost certainly due to variations in their properties. The phase angle dependence of the brightness asymmetry gives an indication as to which property of the aerosols has a dominant role. Theoretical simulations with the aerosol parameters of Rages and Pollack<sup>9</sup> indicate that the contrast declines considerably and even disappears as the phase angle decreases from  $30^\circ$  to  $10^\circ$  for a model involving variations in mean particle size, whereas little contrast alteration is expected over the same range of phase angles for models involving variations in aerosol absorption coefficient or optical depth. Thus the latter models seem to be in better agreement with the observed lack of significant contrast variation with phase angle.

The spectral dependence of the contrast also suggests that it is a reflection of differences in the sub-micrometre aerosol properties rather than differences in albedo of an underlying methane cloud layer. If the contrast was due to an albedo difference deep in the atmosphere it would be attenuated by aerosols in the upper atmosphere. However, to explain the spectral variation of Titan's geometric albedo the visible absorption coefficient of these particles must increase significantly with decreasing wavelength<sup>9</sup>. As their inferred optical depth is higher at shorter wavelengths their attenuation of the north–south contrast of an underlying cloud layer should result in significantly more contrast at long rather than short wavelengths. As this is opposite to the observed spectral vari-

ations, the contrast is more likely to be present in the properties of the sub-micrometre particles in the upper atmosphere.

The large phase shift of the contrast relative to the seasonal forcing functions shows that the contrast-producing mechanism cannot be a direct interaction between the solar irradiance and the atmosphere at the unit optical depth level. A significant depth of Titan's atmosphere must be involved to produce the time delayed response. As a relatively small north–south thermal contrast is expected at levels corresponding to large radiative time constants, a direct thermal effect on the composition or optical depth of the aerosol particles seems unlikely. The observed vertical stability of Titan's temperature profile<sup>10</sup> also argues against an interhemispheric difference in small-scale vertical convection as a modifying influence. This suggests that large-scale circulation asymmetries may be responsible. Possibly differences in meridional circulations, driven by an interhemispheric seasonal thermal contrast, are affecting the aerosol properties by changing the mix of trace gases available at the formation level, or by modifying their rates of removal from the formation region.

### Summary and conclusions

Titan's normal albedo distribution is primarily axially symmetric with a substantial north–south contrast. As the contrast is essentially independent of phase angle it is likely to result from differences in the composition or optical depth of Titan's layer of sub-micrometre aerosols rather than differences in size distribution. The spectral variation of the contrast suggests that it is not caused by differences in the albedo of an underlying methane cloud. The contrast seems to vary with time in response to seasonal variations in solar irradiance and lags the seasonal forcing by a large phase angle, indicating that it originates probably well below the unit optical depth level. It seems to be produced indirectly, perhaps by circulation currents driven by thermal contrast at lower levels which affect the rate of removal or composition of the aerosol particles at the unit optical depth level. The contrast has a significant effect on Titan's disk-integrated brightness, and is probably responsible for most of the observed long term variation, with solar cycle effects accounting for the remainder.

There are still many uncertainties regarding the nature and origin of the contrast. A longer record of observations, both of the contrast and the disk-integrated brightness would yield a significant improvement in understanding. The nature of the contrast variation should be better defined by Voyager 2 observations in August 1981, and by the Space Telescope in the mid-1980s. If the simple seasonal model is correct we would expect the contrast to decrease to zero by the end of 1987.

Continued Earth-based photometry of both Titan and Neptune is also essential to resolve the remaining uncertainties. Between 1972 and 1978 the solar cycle component and the seasonal component have been approximately in phase, and neither has yet experienced a full cycle of variation, making their separate contributions difficult to distinguish from the brightness curves alone. The two components will become readily separated with another 5–10 years of observations as they grow increasingly out of phase, moving in opposite directions between 1981 and 1984.

We thank B. A. Smith and the Voyager imaging team for support, S. A. Collins and J. A. Anderson for help in obtaining the necessary Voyager data, G. W. Lockwood for recent brightness measurements for Titan and Neptune, M. G. Tomasko for normalized Pioneer 11 observations of Titan, and T. Wendricks for drafting the figures. This research was partially supported by JPL contract 953615.

Received 15 June; accepted 9 July 1981.

1. Lockwood, G. W. *Icarus* **32**, 413–430 (1977).
2. Lockwood, G. W. & Thompson, D. T. *Nature* **280**, 43–48 (1979).
3. Suess, S. T. & Lockwood, G. W. *Solar Phys.* **68**, 393–409 (1980).
4. Vidal-Madjar, A. in *The Solar Output and its Variation* (ed. White, O. R.) 213–236 (Colorado Associated University Press, Boulder, 1977).
5. Cook, J. W., Brueckner, G. E. & Van Hoosier, M. E. *J. geophys. Res.* **85**, 2257–2266 (1980).
6. Pollack, J. B., Rages, K. & Toon, O. B. *Geophys. Res. Lett.* **7**, 829–832 (1980).
7. Smith, B. A. *et al.* *Science*, **212**, 163–191 (1981).
8. Toon, O. B., Turco, R. P. & Pollack, J. B. *Icarus* **43**, 260–284 (1980).
9. Rages, K. & Pollack, J. B. *Icarus* **41**, 119–130 (1980).
10. Hanel, R. *et al.* *Science* **212**, 191–200 (1981).
11. *Solar Geophysical Data, prompt reports*, No. 425 (US Dept of Commerce, 1980).